International Journal of Architectural, Civil and Construction Sciences
ISSN: 2415-1734
Vol:11, No:2, 2017

An Advanced Exponential Model for Seismic Isolators Having Hardening or Softening Behavior at Large Displacements

Nicolò Vaiana, Giorgio Serino

***Abstract*—**In this paper, an advanced Nonlinear Exponential Model (NEM), able to simulate the uniaxial dynamic behavior of seismic isolators having a continuously decreasing tangent stiffness with increasing displacement in the relatively large displacements range and a hardening or softening behavior at large displacements, is presented. The mathematical model is validated by comparing the experimental force-displacement hysteresis loops obtained during cyclic tests, conducted on a helical wire rope isolator and a recycled rubber-fiber reinforced bearing, with those predicted analytically. Good agreement between the experimental and simulated results shows that the proposed model can be an effective numerical tool to predict the force-displacement relationship of seismic isolation devices within the large displacements range. Compared to the widely used Bouc-Wen model, unable to simulate the response of seismic isolators at large displacements, the proposed one allows to avoid the numerical solution of a first order nonlinear ordinary differential equation for each time step of a nonlinear time history analysis, thus reducing the computation effort. Furthermore, the proposed model can simulate the smooth transition of the hysteresis loops from small to large displacements by adopting only one set of five parameters determined from the experimental hysteresis loops having the largest amplitude.

***Keywords*—**Base isolation, hardening behavior, nonlinear exponential model, seismic isolators, softening behavior.

I. Introduction

BASE isolation is a widely accepted technique for seismic protection of structures adopting special devices called seismic isolators [1]. There are two common types of seismic isolation bearings, namely, elastomeric and sliding bearings; the former take advantage of the flexible properties of rubber to achieve low horizontal stiffness, whereas the latter rely on the action of sliding to provide horizontal flexibility and on the friction damping occurring at the sliding interface to dissipate energy [2]. Metal devices, such as wire rope isolators, can be used as recentering devices in combination with flat or curved surface sliders [3].

Seismic devices generally exhibit symmetric softening force-displacement hysteresis loops within a relatively large displacements range, that is, under the design earthquake loading. At large displacements, several isolators, such as high damping rubber bearings and wire rope isolators, exhibit a hardening stiffness [4], [5], whereas others, such as unbounded elastomeric bearings, display a softening behavior with a negative tangent stiffness [6].

The differential equation Bouc-Wen model, widely used for modeling the uniaxial behavior of elastomeric bearings, sliding bearings and wire rope isolators within the relatively large displacements range [7]-[9], is unable to efficiently capture their behavior at large displacements [10], [4]. Thus, in this work, a one dimensional (1d) analytical model accommodating the hysteretic behavior at both relatively large and large displacements is proposed. The presented advanced model has been derived by modifying the NEM proposed by [11].

The basic idea is to consider a nonlinear hysteretic exponential element and a nonlinear elastic exponential element connected in parallel. The former stems from the hypothesis that the tangent horizontal stiffness exponentially decreases with increasing displacements within the relatively large displacements range and requires the evaluation of only three parameters, namely, the initial tangent stiffness, the asymptotic tangent stiffness of the relatively large displacements range, and a parameter defining the transition from the initial to the asymptotic tangent stiffness. The latter requires only two parameters and allows to modify the hysteresis loop shape obtained with the hysteretic element so to simulate the increase or decrease of the tangent stiffness at large displacements.

The presented advanced NEM has been validated by comparing the experimental hysteresis loops obtained from horizontal dynamic tests, performed on a helical wire rope isolator and a recycled rubber-fiber reinforced bearing at the Department of Industrial Engineering of the University of Naples Federico II, with those predicted analytically.

II. Proposed Analytical Model

In the first part of this section, the NEM, proposed by [11] to simulate the dynamic behavior of seismic isolators having a continuously decreasing stiffness with increasing displacement in the relatively large displacements range, is presented. This analytical model has been derived by adequately adapting the 1d hysteretic model introduced by [12] to predict the dynamic response of laminated elastomeric bearings under the hypothesis of small strains. In the second part, the proposed NEM is modified to simulate the increase or the decrease of the tangent stiffness at large displacements.

N. Vaiana, PhD Student in Structural and Seismic Engineering, is with the Department of Structures for Engineering and Architecture, University of Napoli Federico II, via Claudio 21, 80125 Napoli, Italy (phone: 0039-329-1876763; e-mail: nicolovaiana@outlook.it).

G. Serino, Full Professor of Structural Engineering, is with the Department of Structures for Engineering and Architecture, University of Napoli Federico II, via Claudio 21, 80125 Napoli, Italy (e-mail: giorgio.serino@unina.it).

A. Nonlinear Exponential Model

Fig. 1 (a) shows the normalized symmetric softening force-displacement hysteresis loop with bilinear characteristics typical of elastomeric bearings, such as high damping rubber bearings and lead rubber bearings, and metal devices, such as wire rope isolators, whereas Fig. 1 (b) presents the normalized symmetric softening force-displacement loop having rigid-plastic characteristics generally displayed by sliding bearings, such as flat sliding bearings. Each hysteresis force-displacement loop can be decomposed into three curves: the first loading curve (portion a-b), namely, virgin curve, the unloading curve (portion b-c), and the loading curve (portion c-d).

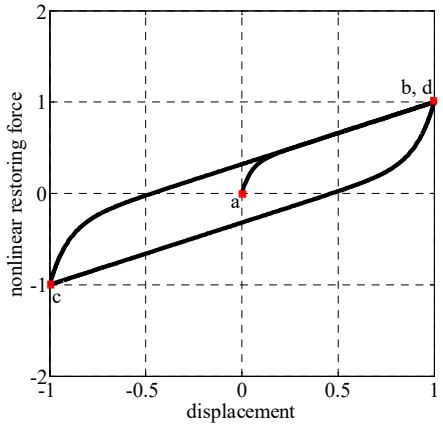

(a)

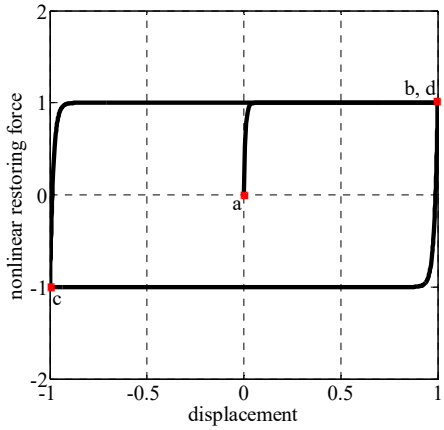

(b)

Fig. 1 Normalized force-displacement loop with (a) bilinear and (b) rigid-plastic characteristics

The loading curve tangent stiffness of the two normalized hysteresis loops shown in Fig. 1 is plotted in Fig. 2 as the function of the horizontal displacement. Since the tangent stiffness functions of the loading and unloading curves are antisymmetric, only the former has been plotted. It can be observed that, in both two cases, the tangent horizontal stiffness exponentially decreases with increasing displacement.

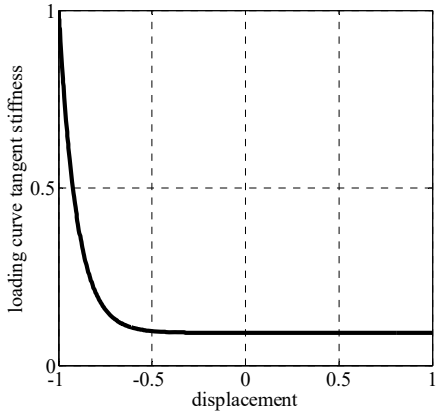

(a)

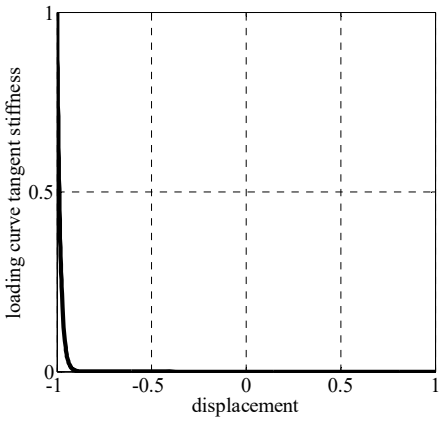

(b)

Fig. 2 Tangent stiffness variation of the loading curve with (a) bilinear and (b) rigid-plastic characteristics

The tangent stiffness $k_t(u)$ can be expressed by the following two mathematical expressions, valid for a loading and an unloading curve, respectively:

$$k_t(u) = k_2 + (k_1 - k_2)\, e^{-a\,(u - u_{min})}, \quad (\dot{u} > 0) \qquad (1)$$

$$k_t(u) = k_2 + (k_1 - k_2)\, e^{-a\,(u_{max} - u)}, \quad (\dot{u} < 0) \qquad (2)$$

where k_1 and k_2 are the initial and the asymptotic values of the tangent stiffness, u_{max} and u_{min} are the horizontal displacement values at the most recent point of unloading and loading, respectively, and a is a parameter that defines the transition from k_1 to k_2.

Integrating (1) and (2), the following nonlinear hysteretic restoring force is obtained:

$$f_h(u) = f_h(u_{\min}) + k_2\,(u - u_{\min}) - \frac{b}{a}\left[e^{-a(u - u_{\min})} - 1\right], \quad (\dot{u} > 0) \quad (3)$$

$$f_h(u) = f_h(u_{\max}) - k_2\,(u_{\max} - u) + \frac{b}{a}\left[e^{-a(u_{\max}-u)} - 1\right],\ (\dot{u} < 0) \quad (4)$$

where $b = k_1 - k_2$. Equations (3) and (4) can be written in a more compacted form as:

$$f_h(u) = f_{lr} + k_2\,(u - u_{lr}) - sgn(\dot{u})\frac{b}{a}\left[e^{-sgn(\dot{u})\,a\,(u-u_{lr})} - 1\right], \quad (5)$$

where $(u_{lr},\ f_{lr})$ is the most recent point of load reversal.

According to Masing's rule, the virgin curve can be obtained applying a similitude transformation of ratio 0.5 to the generic loading or unloading curve of the nonlinear restoring force $f_h(u)$. This means that for a given u on the virgin curve, where u is computed starting from zero, the corresponding tangent stiffness $k_t(u)$ must be equal to the one obtained from the generic loading or unloading curve for a value of $2u$. For this reason, the virgin curve can be evaluated using the following expressions, valid for a loading and an unloading curve, respectively:

$$f_h(u) = k_2\,u - \frac{b}{2a}\left[e^{-2au} - 1\right], (\dot{u} > 0) \quad (6)$$

$$f_h(u) = k_2\,u + \frac{b}{2a}\left[e^{2au} - 1\right]. (\dot{u} < 0) \quad (7)$$

Equations (6) and (7) can be written in a more compacted form as:

$$f_h(u) = k_2\,u - sgn(\dot{u})\frac{b}{2a}\left[e^{-sgn(\dot{u})\,2au} - 1\right]. \quad (8)$$

It is worth to notice that the proposed analytical model requires the evaluation of only three parameters, that is, k_1, k_2, and a, whereas in the widely used uniaxial differential equation Bouc-Wen model [13]-[15], the number of parameters to be identified is equal to seven for both elastomeric and sliding bearings [7], [8]. In addition, the presented model allows to reduce the computational effort of a nonlinear time history analysis by avoiding, for each time step, the numerical solution of the first order nonlinear ordinary differential equation required by the Bouc-Wen model to evaluate the hysteretic variable [16].

B. Advanced NEM

Fig. 3 (a) shows the typical normalized symmetric force-displacement hysteresis loop displayed by seismic isolators having post-hardening behavior at large displacements, such as high damping rubber bearings and wire rope isolators, whereas Fig. 3 (b) shows the typical normalized symmetric force-displacement loop of seismic isolators with post-softening behavior at large displacements, such as unbounded recycled rubber-fiber reinforced bearings.

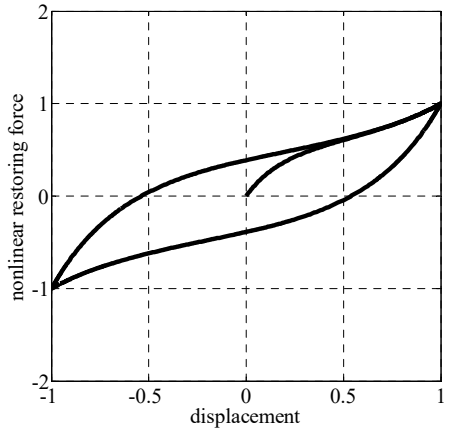

(a)

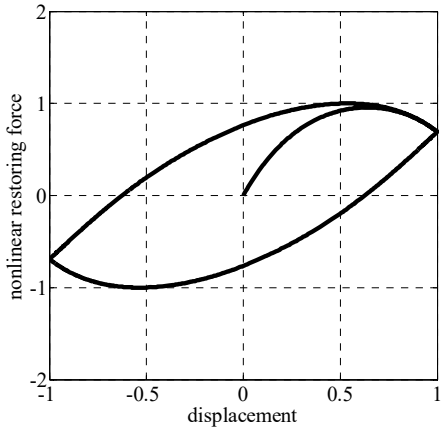

(b)

Fig. 3 Normalized force-displacement loop with (a) post-hardening and (b) post-softening characteristics

The increase or decrease of the tangent stiffness can be simulated by connecting in parallel to the above-described analytical model a nonlinear spring having a tangent stiffness function given by:

$$k_t(u) = c\,[e^{sgn(u)\,d\,u} - 1], \quad (9)$$

where c and d are two parameters of the proposed exponential function. Integrating (9), the following nonlinear elastic force is obtained:

$$f_e(u) = -c\,u + sgn(u)\frac{c}{d}[e^{sgn(u)\,d\,u} - 1]. \quad (10)$$

Hence, the nonlinear total restoring force of the seismic device is given by:

$$f(u) = f_h(u) + f_e(u). \quad (11)$$

Figs. 4 (a) and (b) show the two components of the

nonlinear total restoring force $f(u)$ at large displacements, namely, the nonlinear hysteretic force $f_h(u)$ and the nonlinear elastic force $f_e(u)$, in the case of force-displacement loop with post-hardening and post-softening characteristics, respectively.

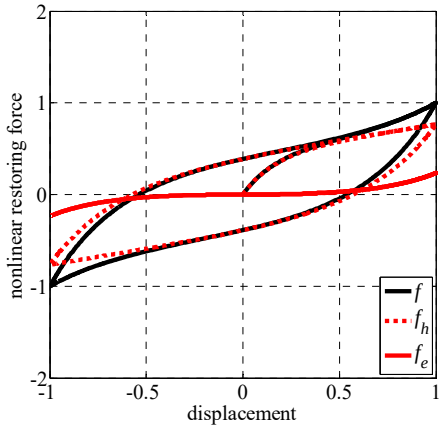

(a)

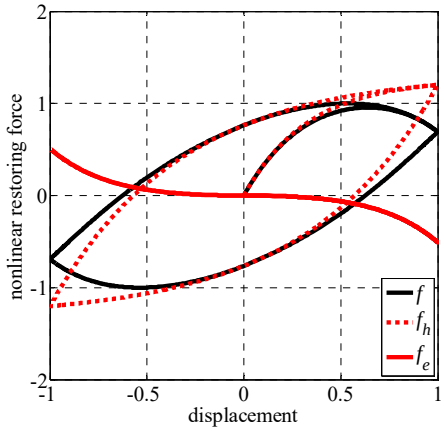

(b)

Fig. 4 Total restoring force components for hysteresis loop with (a) post-hardening and (b) post-softening characteristics

Fig. 5 shows the mechanical model postulated to represent the 1d dynamic response of seismic isolators with hardening or softening behavior at large displacements. The model comprises a uniaxial Nonlinear Hysteretic Spring (NHS) and a uniaxial Nonlinear Elastic Spring (NES) in parallel and two rigid columns representing the height *h* of the bearing.

As it will be shown in the following, the mathematical model expressed by (11) can capture the smooth transition of the hysteresis loops from the relatively large to large horizontal displacement levels by using the same set of five parameters, that is, k_1, k_2, a, c, and d, identified from the experimental loops with the largest amplitude. Finally, it has to be noted that the axial load effects in the isolator device can be accounted for by adjusting the appropriate model parameters.

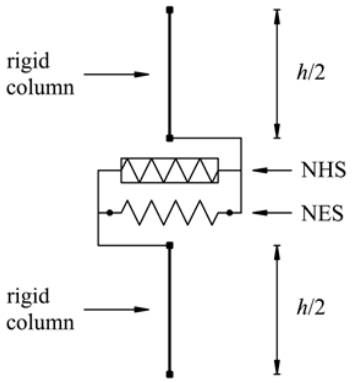

Fig. 5 1d mechanical model

III. Verification of the Proposed Model

In the following, the proposed advanced NEM is validated by comparing the experimental force-displacement hysteresis loops obtained from horizontal dynamic tests, performed on a Helical Wire Rope Isolator (HWRI) and a Recycled Rubber-Fiber Reinforced Bearing (RR-FRB), with those predicted analytically.

A. Testing Machine

Fig. 6 shows the adopted testing machine available at the Department of Industrial Engineering of the University of Naples Federico II (Italy). It consists of a sliding table driven by a horizontal hydraulic actuator, powered by a 75 kW AC electric motor that allows to impose displacement or load histories. The maximum horizontal force is about 50 kN, the maximum speed is 2.2 m/s and the maximum stroke is ± 0.2 m. A vertical hydraulic actuator allows to apply a load up to 190 kN during tests. The experimental apparatus is instrumented in order to measure the relative horizontal displacement between the lower basement and the upper plate, the vertical load and the horizontal load time histories [17].

All tests were conducted by imposing horizontal displacements at room temperature and the data were sampled at 250 Hz.

B. Simulation of the HWRI Dynamic Response

The selected HWRI, manufactured by Powerflex S.r.l. (Limatola, Italy), is made of a wire rope wound in the form of a helix and embedded into two slotted metal retainer bars. The rope of the tested device, constructed by winding a number of strands around an inner core, is made of six strands, each having 25 steel wires, plus a central one with 49 wires. The material of the wires is Stainless Steel Type 316 whereas the material of the two metal bars is aluminum alloy. The geometrical characteristics of the tested HWRI and its two principal horizontal directions, namely, Roll and Shear directions, are shown in Fig. 7.

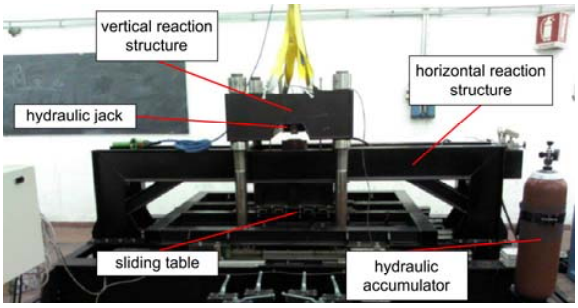

Fig. 6 Testing machine

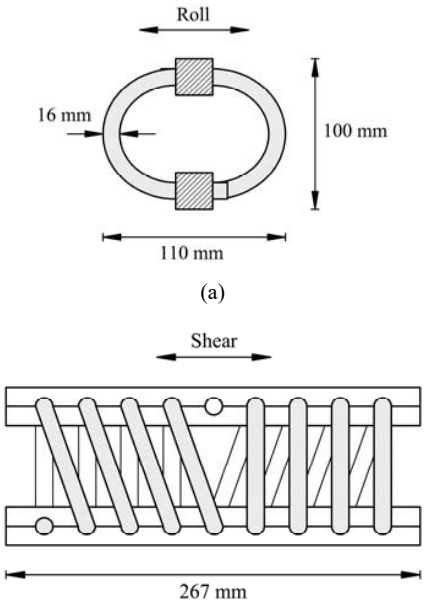

Fig. 7 Geometrical characteristics and principal directions of the tested HWRI: (a) Roll and (b) Shear directions

Adopting the above-described testing machine, a sinusoidal displacement, consisting of five reversed cycles and having frequency f = 1 Hz, was imposed for three different values of amplitude A, that is, 0.25 cm, 0.5 cm, and 1 cm, without and under the effect of a vertical load P_v = 2 kN. According to the experimental tests results, the tested HWRI exhibits a softening behavior in the relatively large displacements range and a post-hardening behavior at large displacements.

Figs. 8-10 give the comparisons of the analytical and experimental results obtained, in both Roll and Shear directions, without the effect of the vertical load, at small (i.e., A = 0.25 cm), relatively large (i.e., A = 0.5 cm), and large (i.e., A = 1 cm) displacements, respectively. It can be observed that the agreement between the experimental and simulated responses is very satisfactory.

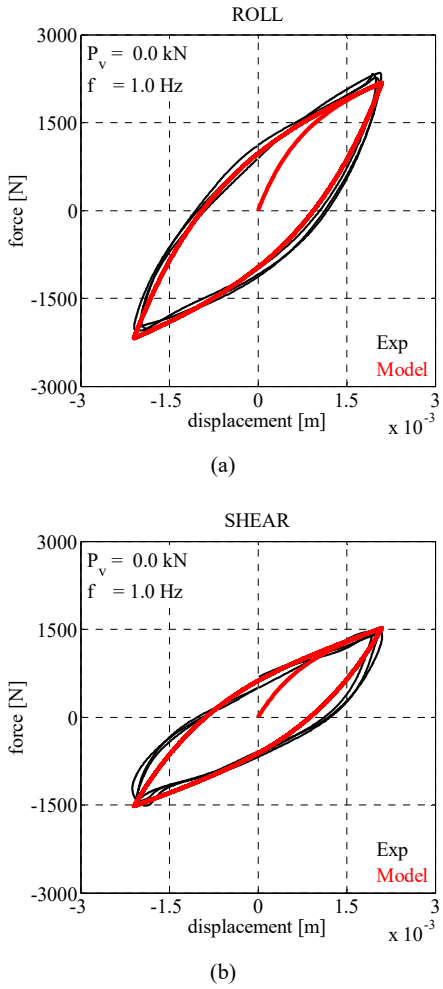

Fig. 8 Analytical and experimental hysteresis loops for A = 0.25 cm: (a) Roll and (b) Shear directions

TABLE I
ANALYTICAL MODEL PARAMETERS

P_v = 0 kN	k_1 [N/m]	k_2 [N/m]	a	c [N/m]	d
Roll	2600000	300000	720	400000	35
Shear	1650000	200000	670	620000	58

The previous force-displacement hysteresis loops have been simulated using the set of five model parameters listed in Table I and determined from the experimental loops having the largest amplitude, that is, A = 1 cm.

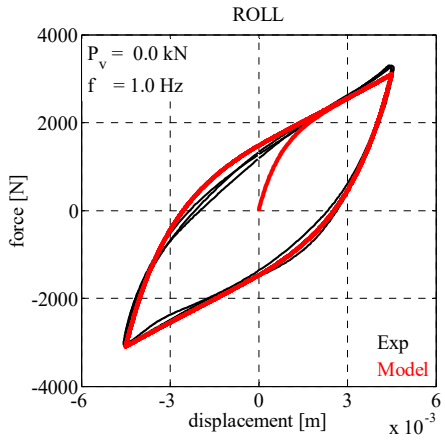

(a)

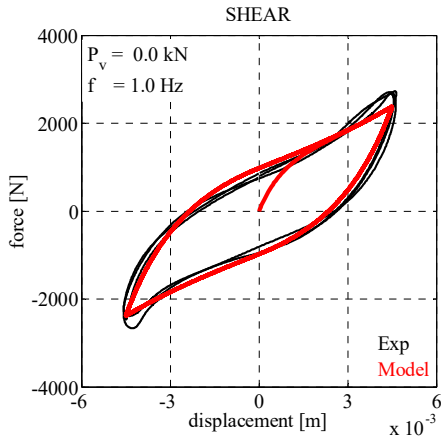

(b)

Fig. 9 Analytical and experimental hysteresis loops for A = 0.5 cm: (a) Roll and (b) Shear directions

Fig. 11 shows the hysteresis force-displacement loops obtained for P_v = 2 kN. In order to account for the effect of the applied vertical load, the five model parameters, listed in Table II, have been adjusted based on the experimental results.

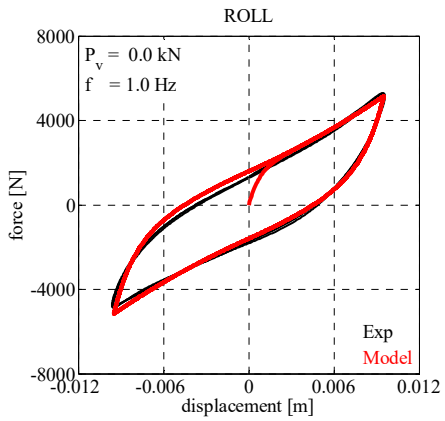

(a)

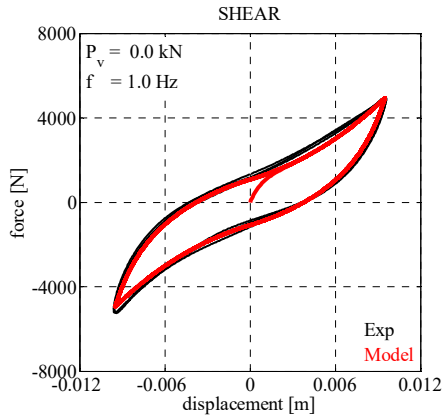

(b)

Fig. 10 Analytical and experimental hysteresis loops for A = 1 cm: (a) Roll and (b) Shear directions

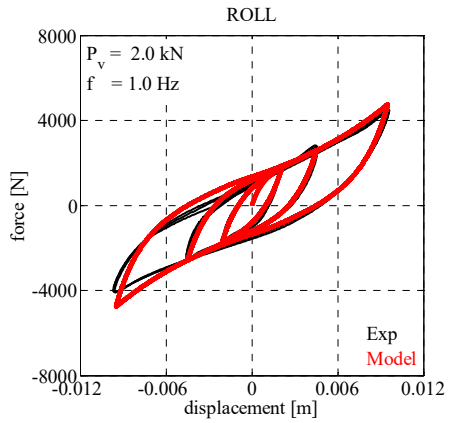

(a)

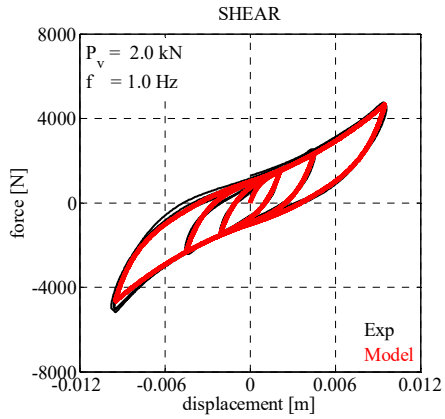

(b)

Fig. 11 Analytical and experimental hysteresis loops for P_v = 2 kN: (a) Roll and (b) Shear directions

TABLE II
ANALYTICAL MODEL PARAMETERS

P_v = 2 kN	k_1 [N/m]	k_2 [N/m]	a	c [N/m]	d
Roll	2100000	220000	710	160000	120
Shear	2000000	220000	900	650000	46

C. Simulation of the RR-FRB Dynamic Response

Fig. 12 shows the tested RR-FRB, manufactured by Isolgomma S.r.l. (Vicenza, Italy), which is made of 12 layers of recycled rubber and 11 high strength quadridirectional carbon fiber fabric sheets used as reinforcing elements. The device is square in plan with dimensions 7 cm x 7 cm and has a total height of approximately 6.3 cm. The equivalent thickness of the carbon fiber layers is 0.007 cm. The shear modulus of the recycled rubber, under the applied vertical load P_v = 16.9 kN, is equal to 1 MPa at 100% shear strain [6].

(a)

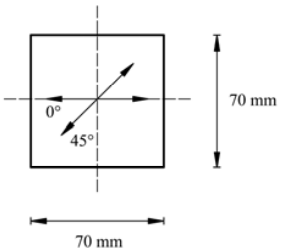

(b)

Fig. 12 (a) Tested RR-FRB and (b) loading directions

The RR-FRB has been tested in unbounded configuration by imposing, in two different horizontal loading directions, namely, 0° and 45° directions (Fig. 12), three cycles of harmonic displacement, having frequency f = 0.87 Hz, under the effect of a constant vertical pressure of 3.45 MPa, for eight different values of amplitude A, that is, 1 cm, 1.5 cm, 2 cm, 2.5 cm, 3 cm, 3.5 cm, 4 cm, and 4.5 cm. According to the experimental tests results, the tested RR-FRB exhibits a softening behavior in the relatively large displacements range and a post-softening behavior at large displacements.

Figs. 13 (a) and (b) show the experimental and simulated hysteresis loops obtained in 0° and 45° loading directions, respectively. It can be noted that a good agreement between the analytical and experimental responses has been obtained.

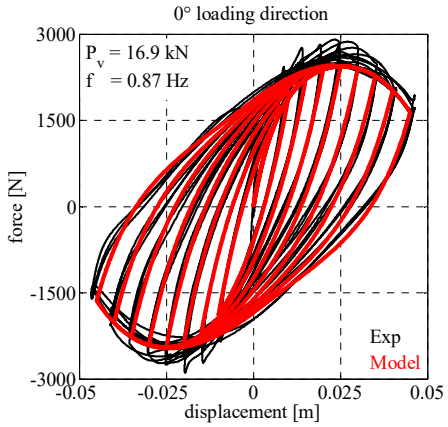

(a)

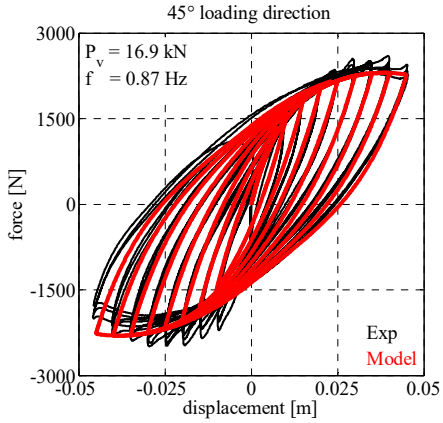

(b)

Fig. 13 Analytical and experimental hysteresis loops in: (a) 0° and (b) 45° loading directions

The previous force-displacement hysteresis loops have been simulated using the set of five model parameters listed in Table III and determined from the experimental loops having the largest amplitude, that is, A = 4.5 cm.

TABLE III
ANALYTICAL MODEL PARAMETERS

P_v = 16.9 kN	k_1 [N/m]	k_2 [N/m]	a	c [N/m]	d
0°	350000	38000	80	-20000	45
45°	250000	40000	70	-70000	12

IV. CONCLUSIONS

An advanced NEM has been proposed to predict the uniaxial dynamic behavior of seismic isolators having hardening or softening behavior at large displacements.

The experimental hysteresis loops obtained from cyclic dynamic tests, performed on a HWRI and a RR-FRB, have been simulated adopting the proposed model in order to demonstrate its accuracy. Good agreement between the analytical and experimental results, at both relatively large and large displacements, has been obtained.

Compared to the widely-used BWM, the proposed one does not require the numerical solution of a nonlinear differential equation for each time step of the analysis, thus decreasing the computational effort. Furthermore, the proposed model is able to capture the smooth transition of the hysteresis loops from the small to the large displacements range using only one set of five parameters evaluated from the experimental hysteresis loops with the largest amplitude.

ACKNOWLEDGMENT

The tested HWRI was manufactured and provided by Powerflex S.r.l. (Limatola, Italy). The authors are grateful to this company and want to thank Prof. Filip C. Filippou for the possibility given to the first author to work on the Simulation of the Seismic Response of Base-Isolated Structures during his research period at the University of California at Berkeley.

REFERENCES

[1] F. Naeim and J. M. Kelly, *Design of Seismic Isolated Structures: From Theory to Practice*. New York: John Wiley & Sons, 1999.
[2] M. C. Constantinou, A. S. Whittaker, Y. Kalpakidis, D. M. Fenz and G. P. Warn, "*Performance of seismic isolation hardware under service and seismic loading*," Technical Report MCEER-07-0012, State University of New York, Buffalo, 2007.
[3] M. Spizzuoco, V. Quaglini, A. Calabrese, G. Serino and C. Zambrano, "Study of wire rope devices for improving the re-centering capability of base isolated buildings," *Structural Control and Health Monitoring*, to be published.
[4] C. S. Tsai, T. C. Chiang, B. J. Chen and S. B. Lin, "An advanced analytical model for high damping rubber bearings," *Earthquake Engineering and Structural Dynamics*, vol. 32, pp. 1373-1387, 2003.
[5] N. Vaiana, M. Spizzuoco and G. Serino, "Influence of displacement amplitude and vertical load on the horizontal dynamic and static behavior of helical wire rope isolators," *Proceedings of the 19th International Conference on Earthquake and Structural Engineering*, London, United Kingdom, 2017.
[6] M. Spizzuoco, A. Calabrese and G. Serino, "Innovative low-cost recycled rubber-fiber reinforced isolator: experimental tests and finite element analyses," *Engineering Structures*, vol. 76, pp. 99-111, 2014.
[7] M. C. Constantinou, A. Mokha and A. M. Reinhorn, "Teflon bearings in base isolation II: modeling," *Journal of Structural Engineering*, vol. 116, no. 2, pp. 455-474, 1990.
[8] S. Nagarajaiah, A. M. Reinhorn and M. C. Constantinou, "Nonlinear dynamic analysis of 3-D base-isolated structures," *Journal of Structural Engineering*, vol. 117, no. 7, pp. 2035-2054, 1991.
[9] G. F. Demetriades, M. C. Constantinou and A. M. Reinhorn, "Study of wire rope systems for seismic protection of equipment in buildings," *Engineering Structures*, vol. 15, no. 5, pp. 321-334, 1993.
[10] Y. Q. Ni, J. M. Ko, C. W. Wong and S. Zhan, "Modelling and identification of a wire-cable vibration isolator via a cyclic loading test. Part 1: experiments and model development," *Journal of Systems and Control Engineering*, vol. 213, no. I3, pp. 163-171, 1999.
[11] N. Vaiana, F. C. Filippou and G. Serino, "Nonlinear dynamic analysis of base-isolated structures using a partitioned solution approach and an exponential model," *Proceedings of the 19th International Conference on Earthquake and Structural Engineering*, London, United Kingdom, 2017.
[12] G. Serino, "*Modelli per la determinazione delle proprietà meccaniche degli isolatori elastomerici armati*," Convenzione di ricerca con l'ENEL/DSR/CRIS, Rapporto Tecnico fase 1/94, Napoli, 1994.
[13] R. Bouc, "Modele mathematique d'hysteresis," *Acustica*, vol. 24, pp. 16-25, 1971.
[14] Y. K. Wen, "Method for random vibration of hysteretic systems," *Journal of the Engineering Mechanics Division*, vol. 102, no. EM2, pp 249-263, 1976.
[15] Y. K. Wen, "Equivalent linearization for hysteretic systems under random excitation," *Journal of Applied Mechanics*, vol. 47, pp 150-154, 1980.
[16] N. Vaiana and G. Serino, "Speeding up nonlinear time history analysis of base-isolated structures using a nonlinear exponential model," *Proceedings of the 19th International Conference on Earthquake Engineering*, Barcelona, Spain, 2017.
[17] S. Pagano, M. Russo, S. Strano and M. Terzo, "A mixed approach for the control of a testing equipment employed for earthquake isolation systems," *Journal of Mechanical Engineering Science*, vol. 228, no. 2, pp. 246-261, 2014.